Lipocalin 2 induces visual impairment by promoting ferroptosis in retinal ischemia-reperfusion injury

Tingfang Mei[1]^, Jinwen Wu[1], Keling Wu[1], Minglei Zhao[1], Jingyi Luo[1], Xinqi Liu[1,2], Bizhi Shang[1], Wenchang Xu[1], Zeqiu Yang[1], Yuhua Lai[1], Chujun Liu[1], Haijun Gong[1,3], Xinbo Gao[1], Yehong Zhuo[1], Mingkai Lin[1], Ling Zhao[1]^

[1]State Key Laboratory of Ophthalmology, Zhongshan Ophthalmic Center, Sun Yat-sen University, Guangdong Provincial Key Laboratory of Ophthalmology and Visual Science, Guangzhou, China; [2]Guangdong Province Key Laboratory of Brain Function and Disease, Zhongshan School of Medicine, Sun Yat-sen University, Guangzhou, China; [3]Department of Ophthalmology, Guangdong Provincial Key Laboratory of Malignant Tumor Epigenetics and Gene Regulation, Sun Yat-sen Memorial Hospital, Sun Yat-sen University, Guangzhou, China

Contributions: (I) Conception and design: L Zhao, T Mei; (II) Administrative support: None; (III) Provision of study materials or patients: L Zhao, T Mei, J Wu, C Liu, Y Lai, H Gong, X Gao, Y Zhuo, M Lin; (IV) Collection and assembly of data: L Zhao, T Mei, J Wu, K Wu, M Zhao, J Luo; (V) Data analysis and interpretation: L Zhao, T Mei, X Liu, B Shang, W Xu, Z Yang, H Gong, X Gao, Y Zhuo, M Lin; (VI) Manuscript writing: All authors; (VII) Final approval of manuscript: All authors.

Correspondence to: Prof. Ling Zhao. State Key Laboratory of Ophthalmology, Zhongshan Ophthalmic Center, Sun Yat-sen University, Guangdong Provincial Key Laboratory of Ophthalmology and Visual Science, 7 Jinsui Road, Tianhe District, Guangzhou, China. Email: zhaoling6@mail.sysu.edu.cn.

Background: Retinal ischemia-reperfusion (RIR) is a common pathological condition that can lead to retinal ganglion cell (RGC) death and visual impairment. However, the pathogenesis of RGC loss and visual impairment caused by retinal ischemia remains unclear.

Methods: A mouse model of elevated intraocular pressure (IOP)-induced RIR injury was used. Flash visual evoked potentials (FVEPs) and electroretinography (ERG) recordings were performed to assess visual function. The structural integrity of the retina and the number of RGC were assessed using hematoxylin and eosin (HE) staining and retinal flat mounts. Ferroptosis was evaluated by testing the levels of glutathione (GSH), malondialdehyde (MDA), glutathione peroxidase (GPX4), and ferritin light chains (FTL) in the retina of wild-type (WT) and lipocalin-2 transgenic (*LCN2-TG*) mice after RIR injury.

Results: We found that LCN2 was mainly expressed in the RGC layer in the retina of wild-type mice and remarkably upregulated after RIR injury. Compared with wild-type mice, aggravated RGC death and visual impairment were exhibited in *LCN2-TG* mice with RIR injury. Moreover, LCN2 overexpression activated glial cells and upregulated proinflammatory factors. More importantly, we found that LCN2 strongly promoted ferroptosis signaling in RGC death and visual impairment. Liproxstatin-1, an inhibitor of ferroptosis, could significantly ameliorate RGC death and visual impairment. Furthermore, we found significantly alleviated RGC death and retinal damage in LCN2 heterozygous knockout mice.

Conclusions: Our study provides important insights linking upregulated LCN2-mediated promotion of ferroptosis to RGC death and visual function impairment in the pathogenesis of ischemic retinopathy.

Keywords: Lipocalin-2 (LCN2); retinal ischemia-reperfusion injury (RIR injury); ferroptosis; retinal ganglion cell (RGC); visual impairment

---

^ ORCID: Tianfang Mei, 0000-0002-9904-7444; Ling Zhao, 0000-0002-6644-2886.

Page 2 of 15

Mei et al. LCN2 promotes ferroptosis in ischemic retinopathy

Introduction

Retinal ischemia-reperfusion (RIR) occurs in a variety of visual impairment eye diseases. RIR is characterized by initial restriction of the blood supply and subsequent resumption of reperfusion. It is a common pathological condition involved in various ocular disorders, including acute glaucoma, retinopathy of prematurity, ischemic optic neuropathy, and diabetic retinopathy (1-3). However, it is well known that RIR can lead to retinal ganglion cell (RGC) death and visual impairment (4,5). However, the molecular mechanism of RGC death and associated therapeutic targets remain unclear.

Ferroptosis is characterized by lipid peroxidation and dependence on irons, which differs from apoptosis, necrosis, and autophagic cell death (6,7). Ferroptosis can be induced by the inhibition of glutathione peroxidase 4 (GPX4) (8,9). Significant downregulation of GPX4 and increased lipid peroxidation-induced ferroptosis are associated with multiple neurodegenerative diseases, such as Parkinson and Alzheimer diseases (10,11). Recent studies reported that deferoxamine, an iron chelator, is protective against RGC loss in the microbead occlusion model of ocular hypertension, and ferroptosis is involved in the process of RIR in mice (12,13). However, the molecular mechanism underlying ferroptosis and RGC death in RIR models still needs to be explored.

Lipocalin-2 (LCN2), also known as neutrophil gelatinase-associated lipocalin or 24p3, is a small, secreted protein that belongs to the lipocalin protein family. LCN2 plays important roles in immune response, cell migration and proliferation, iron transport, cell differentiation, and cell death (14,15). Numerous studies have reported that LCN2 is significantly upregulated in various ischemic-reperfusion-injured tissues, including renal and cerebral ischemia-reperfusion injury (16,17). However, the mechanism by which LCN2 regulates RGC death from RIR injury remains largely unknown.

In this study, we examined the connection between LCN2 and ferroptosis and clarified their relationships with RGC death and visual function impairment. Our findings demonstrate that elevated LCN2 aggravates RGC death by promoting retinal ferroptosis in the progression of RIR injury. In doing so, our study contributes to improving the understanding of the pathogenesis of retinal ischemia. We present the following article in accordance with the ARRIVE reporting checklist (available at https://atm.amegroups.com/article/view/10.21037/atm-22-3298/rc).

Methods

Experimental model

C57BL/6J wild-type (WT) mice (4-6 weeks old, specific pathogen-free), LCN2 transgenic (*LCN2-TG*) mice, and LCN2 heterozygous knockout mice produced on a C57BL/6J genomic background were purchased from GemPharmatech Co., Ltd. (Jiangsu, China). Animals were housed in the Animal Laboratory of Zhongshan Ophthalmic Center under a 12-h light-dark cycle, with free access to food and water before use. Mice were randomly allocated to 4 groups: (I) the normal group, containing mice without any injury in the left eyes of the mice; (II) the RIR injury group, containing mice with RIR induced by elevated intraocular pressure (IOP) in the right eyes of the mice; (III) the vehicle group, containing mice intraperitoneally injected with 1% dimethyl sulfoxide (DMSO) in phosphate-buffered saline (PBS); and (IV) the liproxstatin-1-treated group, containing mice intraperitoneally injected with liproxstatin-1 (liproxstatin-1, 10 mg/kg; S7699; Selleck Chemicals, Houston, TX, USA). During the different stages of the experiment, the researchers were aware of the group allocation. Each group contained 6 eyes for each experimental project. All animal procedures were conducted according to Association for Research in Vision and Ophthalmology (ARVO) Statement for the use of Animals in Ophthalmic and Vision Research. Experiments were performed under a project license (No. 2020-070) granted by the Institutional Ethics Committee of the Zhongshan Ophthalmic Center, Sun Yat-sen University, in compliance with its guidelines for the care and use of animals.

Elevated IOP-induced RIR injury model

The RIR injury model was established as previously described (18). Four- and six-week-old mice, weighing 16 to 20 g, were anesthetized by intraperitoneal injection with 50 mg/kg of pentobarbital sodium. The corneas were dropped with 0.5% tetracaine hydrochloride for local anesthesia, and the pupils were dilated with 1% tropicamide eye drops. Then, a 30-gauge needle connected to a balanced saline solution with a height of 150 cm was cannulated into the anterior chamber in the right eye. IOP was elevated to 110 mmHg for 60 minutes. The contralateral eye served as the control. The needle was withdrawn afterward to allow for natural retinal reperfusion, and tobramycin ointment was applied to the eyes to prevent bacterial infection.

Liproxstatin-1 administration

Mice were randomly divided into the control group (vehicle; 1% DMSO in PBS) and the experimental group (liproxstatin-1, 10 mg/kg; S7699; Selleck Chemicals) (19,20). Mice were intraperitoneally injected with liproxstatin-1 (LPX-1) or the vehicle an hour before RIR injury.

Histological examination

Five days after the RIR injury, mice were killed, and their eyes were collected, fixed with fresh 4% paraformaldehyde overnight, and embedded in paraffin. Each paraffin section (5 μm thick) was stained with hematoxylin and eosin (HE). The total thickness of the retina from the inner limiting membrane to the outer limiting membrane was measured within 1 mm of the optic nerve.

Immunofluorescence staining

The mice were anesthetized with pentobarbital sodium, and their eyes were isolated and immersed in fresh 4% paraformaldehyde for an hour and dehydrated gradually in sucrose. The eyeballs were embedded in optimum cutting temperature (OCT), frozen, and sliced into 8 μm thick sections. The retinal sections were permeabilized and blocked with 0.5% Triton X-100 and 5% bovine serum albumin (BSA) in PBS for an hour at room temperature. Then, the sections were incubated with rabbit anti-LCN2 antibody (1:100; Cat#38356; Signalway Antibody), mouse anti-Brn3a antibody (1:100; Cat#MAB1585; MilliporeSigma, Burlington, MA, USA), rabbit anti-FTL antibody (1:100; Cat#10727; Proteintech, Rosemont, IL, USA), rabbit anti-glial fibrillary acidic protein (GFAP) antibody [1:200; Cat#12389; Cell Signaling Technology (CST), Danvers, MA, USA], rabbit polyclonal anti-IBA-1 antibody (1:200; Cat#019-19741 Wako Chemicals, Richmond, VA, USA), and rat anti-CD68 antibody (1:200; Cat#MCA1957; BD Biosciences, Franklin Lake, NJ, USA) overnight at 4 ℃. The frozen sections were incubated with corresponding secondary antibodies for 2 hours at room temperature. Nuclei were stained with 4',6-diamidino-2-phenylindole (DAPI) (1:1,000; Cat#D8417; Sigma-Aldrich, St. Louis, MO, USA) for 5 min under darkness. The fluorescence images were obtained from a confocal microscope (LSM980; Carl Zeiss, Oberkochen, Germany).

RGC labeling for retinal flat mounts

Mice were intraperitoneally anesthetized with 50 mg/kg of pentobarbital sodium 5 days after RIR injury. Their eyeballs were obtained and fixed in 4% paraformaldehyde for 40 min. The retina was acquired after peeling the cornea, sclera, and lens using forceps. The retina samples were permeabilized and blocked with 0.5% Triton X-100 and 5% BSA in PBS overnight at 4 ℃. Then, the samples were incubated with rabbit anti-RNA-binding protein with multiple splicing (RBPMS) antibody (1:200; AB152101; Abcam, Cambridge, UK) for 48 h at 4 ℃. Donkey anti-rabbit immunoglobin G (IgG; H + L) secondary antibody to Alexa Fluor 555 was added for 2 hours at room temperature, and the retina was washed in PBS 3 times after each incubation. Then, the retinal flat mount images were examined under a TissueFAXS (TissueGnostics, Vienna, Austria). Quantification of RGC was performed for a 200×200 μm area in 12 areas captured from the peripheral, middle, and central areas of the retina and averaged for retinas per each control and experimental condition. The orientation was shown as S (superior), I (inferior), N (nasal), and T (temporal).

Electroretinography (ERG)

ERG responses were recorded for WT and *LCN2-TG* mice using an Espion V6 system (Diagnosys, Lowell, MA, USA). The mice were dark-adapted overnight and intraperitoneally anesthetized with 50 mg/kg of pentobarbital sodium under red light 5 days after RIR injury. We used 1% tropicamide to dilate the pupil. ERG recordings were obtained simultaneously from both eyes using gold wire loop electrodes. ERG responses (a- and b-waves acquisitions) were obtained with light intensities of 1 cd·s/m^2 under dark-adapted conditions. For the acquisition of c-waves, the eyes were flashed with light intensities of 150 cd·s/m^2 for 100 ms.

Flash visual evoked potentials (FVEPs)

FVEPs were performed on the Celeris apparatus (Diagnosys) to evaluate the RGC function. Mice were dark-adapted overnight and intraperitoneally anesthetized with 50 mg/kg of pentobarbital sodium 5 days after RIR injury. The eyes of the mice were dilated with 1% tropicamide eye drops. Mice were placed on the heated surface of the

Page 4 of 15

Mei et al. LCN2 promotes ferroptosis in ischemic retinopathy

Celeris system to maintain their body temperature. Needle electrodes were placed subcutaneously in the snout, tail, and back of the head at the location of the visual cortex. Each eye was separately exposed to white light flashes of 0.05 cd·s/m^2 and swept 100 times per trial. White light through the corneal stimulators and responses in the visual cortex were recorded for 300 ms at 2,000 Hz.

Glutathione (GSH) and malondialdehyde (MDA) assays

Five days after RIR injury, the retinal samples were collected for GSH or MDA analysis using a GSH and oxidized glutathione (GSSG) Assay Kit or Lipid Peroxidation MDA Assay Kit (Beyotime Biotechnology, Shanghai, China) according to the manufacturer's instructions. Data were normalized to the weight of the tissues.

Western blotting

Total protein was obtained from retinal tissue on the fifth day after RIR injury. Radio-immunoprecipitation assay (RIPA) lysis buffer (Beyotime Biotechnology, Shanghai, China) containing protease and phosphatase inhibitor (Beyotime Biotechnology, Shanghai, China) was added into dissected retinas. Protein samples were separated by a 10-12% SDS-PAGE gel (Beyotime Biotechnology, Shanghai, China) and transferred to polyvinylidene difluoride (PVDF) membranes (MilliporeSigma, Burlington, MA, USA). The PVDF membranes were blocked with 5% BSA in tris-buffered saline with Tween 20 (TBST) for 2 hours at room temperature and incubated at 4 ℃ overnight with primary antibodies. Primary antibodies consisted of goat anti-LCN2 antibody (1:1,000; Cat#AF1857; R&D Systems, Minneapolis, USA), GPX4 (1:1,000; Cat#67763-1-lg; Proteintech), and β-tubulin (1:2,000; Cat#2146; CST). Subsequently, membranes were incubated with corresponding secondary antibodies (1:5,000) for 2 hours at room temperature, and the blots were shown with an enhanced chemiluminescence (ECL) kit (Thermo Fisher Scientific, Waltham, MA, USA) and visualized with an Image Lab imaging system (Uvitec, Cambridge, UK). The protein levels were normalized to tubulin and expressed relative to the WT or control.

Quantitative real-time reverse transcription polymerase chain reaction and quantitative polymerase chain reaction

Total RNA extraction from the retinal tissue with TRIzol Reagent (Invitrogen, Thermo Fisher Scientific, Waltham, MA, USA) was conducted according to the manufacturer's instructions and as previously described (21). Complement DNA (cDNA) was synthesized using ReverTra Ace qPCR RT Master Mix with gDNA Remover (Toyobo, Osaka, Japan). Quantitative polymerase chain reaction (qPCR) was performed with a CFX Connect Real-Time PCR Detection System (Bio-Rad Laboratories, Hercules, CA, USA). Relative messenger RNA (mRNA) expression levels were normalized to glyceraldehyde 3-phosphate dehydrogenase (*GADPH*) control and expressed relative to the WT. The qPCR primer sequences of the target genes are listed in Table S1.

Statistical analysis

Data are shown as the mean ± standard error of the mean (SEM). Each experiment was repeated at least 3 times. Significant differences between 2 groups were analyzed using a 2-tailed unpaired *t*-test performed with GraphPad Prism software (version 8.0; GraphPad Software, La Jolla, CA, USA). A P value less than 0.05 was considered statistically significant.

Results

Upregulation of LCN2 expression in the retina after RIR injury

To explore whether LCN2 is involved in the pathological process of ischemic retinopathy, we used a mouse model of IOP-induced RIR injury. First, we examined the protein levels of LCN2 at different time points (1, 3, and 5 days) after RIR injury. Western blot analysis showed that the protein level of LCN2 was significantly elevated after RIR injury in WT mice (*Figure 1A,1B*). The upregulation of LCN2 in the retina suggested that LCN2 might be involved in the modulation of RIR injury. To further determine the role of upregulated LCN2 in the RIR injury model, we used an *LCN2* transgenic (*LCN2-TG*) mouse model with inserted human *LCN2* CDS (Figure S1). Compared with the those of WT mice, the retinas of *LCN2-TG* mice showed an increased level of LCN2, as verified by Western blot (*Figure 1C,1D*; Figure S2). We used immunostaining of LCN2 to examine its distribution in mice retinas. In the retinas of WT mice, LCN2 was mainly expressed in the ganglion cell layer (GCL; *Figure 1E*). However, in the retina of *LCN2-TG* mice, LCN2 was not only expressed in the GCL but also in the retinal inner plexiform layer (IPL),
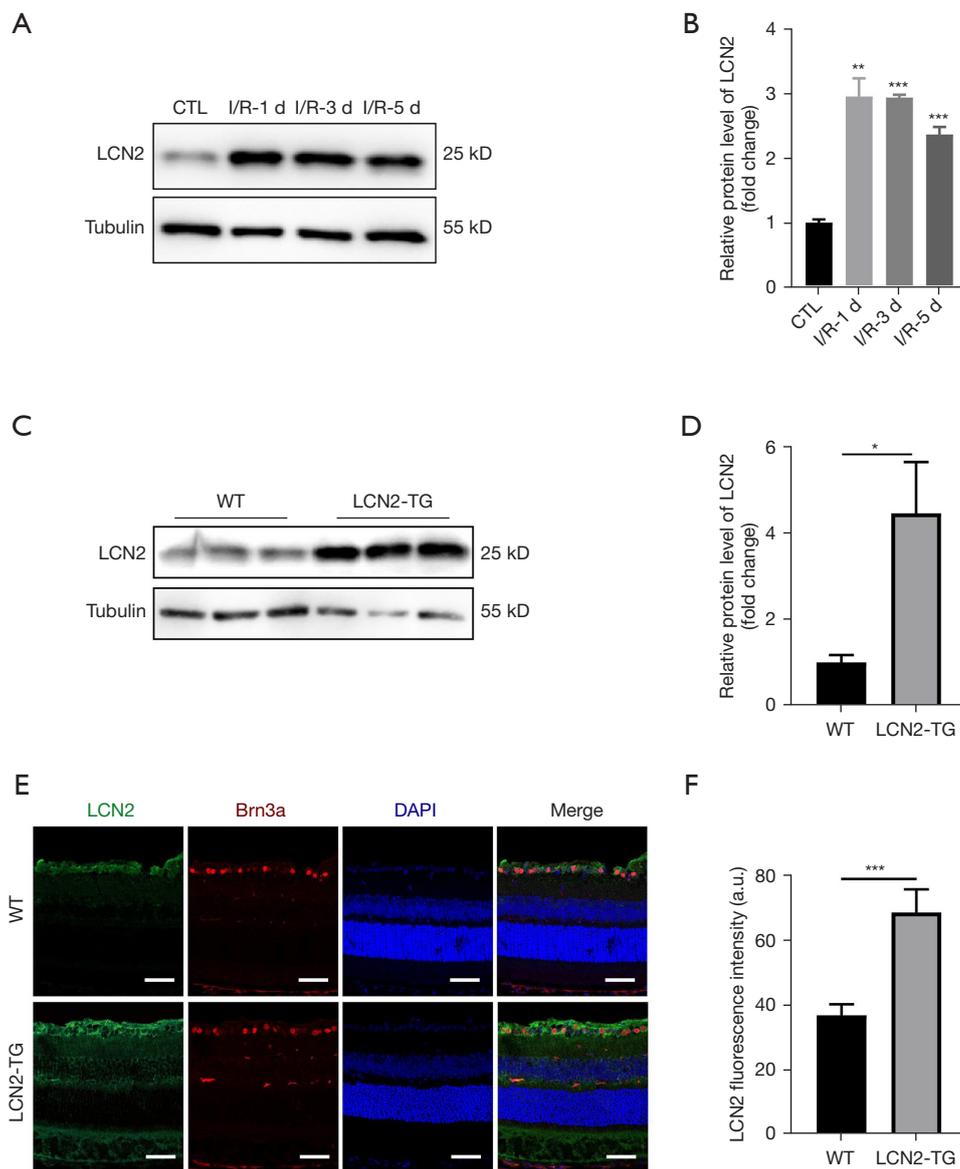
Figure 1 Upregulation of LCN2 in the retina after retinal ischemia-reperfusion injury. (A,B) Western blot analysis showed elevated LCN2 expression levels at different time points (1, 3, and 5 days) after RIR injury. Statistical analysis was performed with an unpaired 2-tailed Student *t*-test. n=3 mice per group. All data represent the mean ± SEM. **, P<0.01; ***, P<0.001. (C,D) The LCN2 expression of *LCN2-TG* mice in the retinas was detected using Western blotting. n=3 mice per group. All data represent the mean ± SEM. *, P<0.05. (E) Immunofluorescence images showed the expression and location of LCN2 in the retinas of WT and LCN2-TG mice. Scale bar: 50 μm. (F) LCN2 fluorescence quantification measurements in the retinal ganglion cell layer. n=3 mice per group. All data represent the mean ± SEM. ***, P<0.001. CTL, control; I/R, ischemia/reperfusion; LCN2, lipocalin-2; *LCN2-TG*, LCN2 transgenic; DAPI, 4',6-diamidino-2-phenylindole; SEM, standard error of the mean.

inner nuclear layer (INL), outer plexiform layer (OPL), and photoreceptor layer (*Figure 1E*). The level of LCN2 was significantly elevated in the RGC layer of *LCN2-TG* mice

(*Figure 1F*). Thus, our study found that the expression of LCN2 was remarkably elevated after the RIR injury model, and the *LCN2-TG* mice were used for further investigation.

Page 6 of 15

Mei et al. LCN2 promotes ferroptosis in ischemic retinopathy

Overexpressed LCN2 exacerbated RGC death and visual impairment after RIR injury

To identify the effects of LCN2 in the RIR injury model, we performed HE staining to assess the pathological change in the retinas of both WT and *LCN2-TG* mice after RIR injury. Before RIR injury, no significant differences were found in total retinal thickness between WT and *LCN2-TG* mice. However, 5 days after RIR injury, we found that total retinal thickness was significantly decreased in *LCN2-TG* mice compared with WT mice (*Figure 2A,2B*). The number of RGC was evaluated by RBPMS staining of retinal flat mounts (22). RBPMS contains one RNA recognition motif (RRM) domain and belongs to the RRM family of RNA-binding proteins. RBPMS has been previously identified as a specific marker for RGC (23). Compared with WT mice, the number of RGCs significantly decreased in *LCN2-TG* mice after RIR injury (*Figure 2C,2D*).

We next examined the FVEPs in the eyes of the control groups (WT and *LCN2-TG*) and the RIR injury groups (WT and *LCN2-TG*). FVEP stimuli elicited prominent responses in the eyes of both WT and *LCN2-TG* mice (the control group), whereas FVEPs were markedly decreased in the eyes of *LCN2-TG* mice (the RIR injury group) compared with the eyes of WT mice (the RIR injury group; *Figure 2E,2F*). In addition, the a-, b-, and c-wave amplitudes of scotopic ERGs from WT and *LCN2-TG* mice were examined to assess retinal function. Compared with WT mice, the amplitudes of the a-waves and c-waves showed no significant difference, but the amplitude of b-waves was severely reduced after RIR injury in *LCN2-TG* mice (Figure S3). These findings demonstrated that upregulated LCN2 exacerbated retinal damage and exerted more harmful effects in the RIR injury model.

Upregulated LCN2 facilitated retinal ferroptosis in the RIR injury model

Ferroptosis is an iron-dependent regulated cell death mechanism (24). To verify the hypothesis that elevated LCN2 can promote retinal ferroptosis and aggravate RGC loss after RIR injury in *LCN2-TG* mice, we quantified the levels of ferroptosis and lipid peroxidation markers, including GSH, MDA, and ferritin light chains (FTL), along with GPX4. GSH is an essential intracellular antioxidant in aerobic cells (25) and is also regarded as an important regulator of ferroptosis (6,26). Compared with WT mice, notably decreased total GSH contents were detected in

LCN2-TG mouse retinas after RIR injury (*Figure 3A*). Lipid peroxidation accumulation is another major hallmark of ferroptotic cell death progression (27). The increased oxidative stress can cause oxidative damage in the retinas as measured by quantifying MDA (28). A significantly increased MDA level was seen in *LCN2-TG* mouse retinas compared with WT mice after RIR injury (*Figure 3B*). GPX4 is a critical antioxidant enzyme that detoxifies various lipid peroxides in cell membranes (29). Therefore, we further determined the protein level of retinal GPX4 under RIR injury. Compared with WT mice, the *LCN2-TG* mice showed a significantly decreased protein level of GPX4 (*Figure 3C,3D*). Ferritin is the main intracellular iron storage protein composed of ferritin heavy chains (FTH1) and FTLs (30). Ferritin plays a key role in protecting against ferroptosis. The level of FTL decreased significantly after RIR injury in *LCN2-TG* mice compared with WT mice (*Figure 3E,3F*). These results indicated that elevated LCN2 could trigger retinal ferroptosis in the RIR injury model.

Upregulated LCN2 promoted activated glial cells and aggravated inflammatory responses

LCN2 can induce activation of astrocytes and microglia and exacerbate the liposaccharide (LPS)-induced neuroinflammation response (31,32). Therefore, we then examined whether LCN2 could trigger the RIR injury-induced elevation of proinflammatory factors in the retinas. GFAP is a marker for astrocytes and activated Müller glial cells in the retina (33). Double immune staining for cellular retinaldehyde-binding protein (CRALBP) and GFAP was used to detect the activation of Müller cells in retinas. Our data showed that the elevation of LCN2 promoted the activation of Müller cells in *LCN2-TG* mice compared with WT mice after RIR injury (*Figure 4A*; Figure S4A). Meanwhile, in WT and *LCN2-TG* mice retinal section samples, we also detected the expression of activated microglia labeled with anti-IBA1 and anti-CD68 antibodies. Compared with WT mice, the IBA1 and CD68 were markedly elevated in the retinas of *LCN2-TG* mice after RIR injury (*Figure 4B*; Figure S5A). We next determined whether the induced elevation of mRNA expression levels of inflammatory cytokines and chemokines in the retina was caused by overexpressed LCN2. As expected, we observed significantly elevated expression levels of interleukin 1 beta (IL-1β), IL-6, C-C motif chemokine ligand 2 (CCL2), and CCL3 in *LCN2-TG* mice compared with WT mice after RIR injury (*Figure 4C-4F*). These results showed that
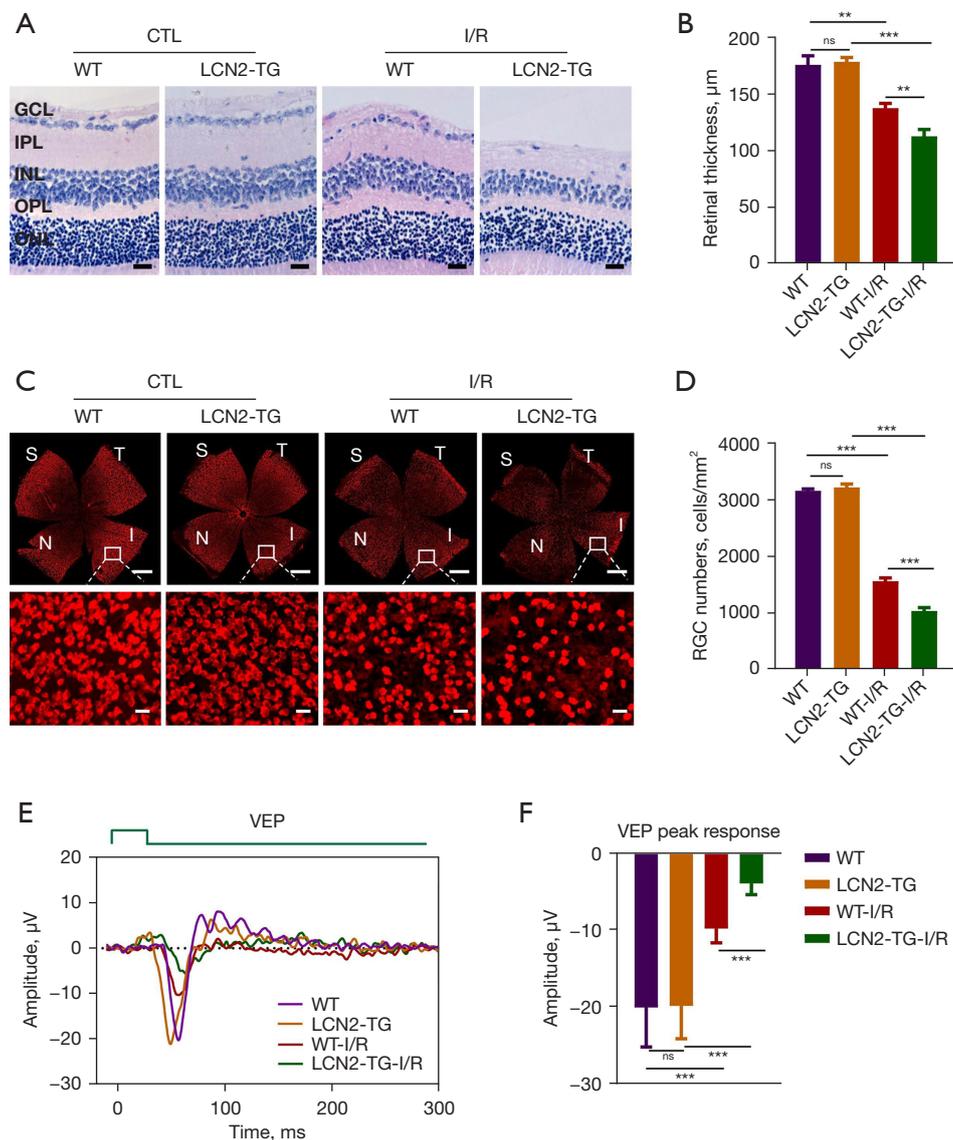
Figure 2 Overexpressed LCN2 exacerbated retinal ganglion cell death and visual impairment after RIR injury. All samples were collected from the retinas 5 days after RIR injury. (A,B) Hematoxylin and eosin staining of paraffin sections showed that overexpression LCN2 aggravated tissue damage and decreased retinal thickness compared with WT mice. Scale bar: 20 μm. n=5 mice per group. All data represent the mean ± SEM. **, P<0.01; ***, P<0.001; ns, no significance. (C) Overexpression of LCN2 decreased RGC numbers in response to RIR injury, as shown using red dots in retinal flat mounts. RGCs were immunostained with an anti-RBPMS antibody. Scale bar: 500 μm (top). Scale bar: 20 μm (bottom). (D) Quantification of RGC was performed for a 200×200 μm area in 12 areas captured from the peripheral, middle, and central areas of the retina and averaged for retinas per each control and experimental condition. n=6 mice per group. All data represent the mean ± SEM. ***, P<0.001; ns, no significance. (E,F) VEPs of WT and *LCN2-TG* mice in left eyes (without RIR injury) and in right eyes (with RIR injury). E shows the representative individual response, while F shows the amplitudes of the VEPs response peaks. n=6 mice per group. All data represent the mean ± SEM. ***, P<0.001; ns, no significance. Statistical analysis was performed with an unpaired 2-tailed Student *t*-test. CTL, control; WT, wild-type; LCN2, lipocalin-2; LCN2-TG, LCN2 transgenic; S, superior; I, inferior; N, nasal; T, temporal; GCL, ganglion cell layer; IPL, inner plexiform layer; INL, inner nuclear layer; OPL, outer plexiform layer; ONL, outer nuclear layer; I/R, ischemia/reperfusion; VEP, visual evoked response; RIR, retinal ischemia-reperfusion; SEM, standard error of the mean; RGC, retinal ganglion cell; RBPMS, RNA-binding protein with multiple splicing.
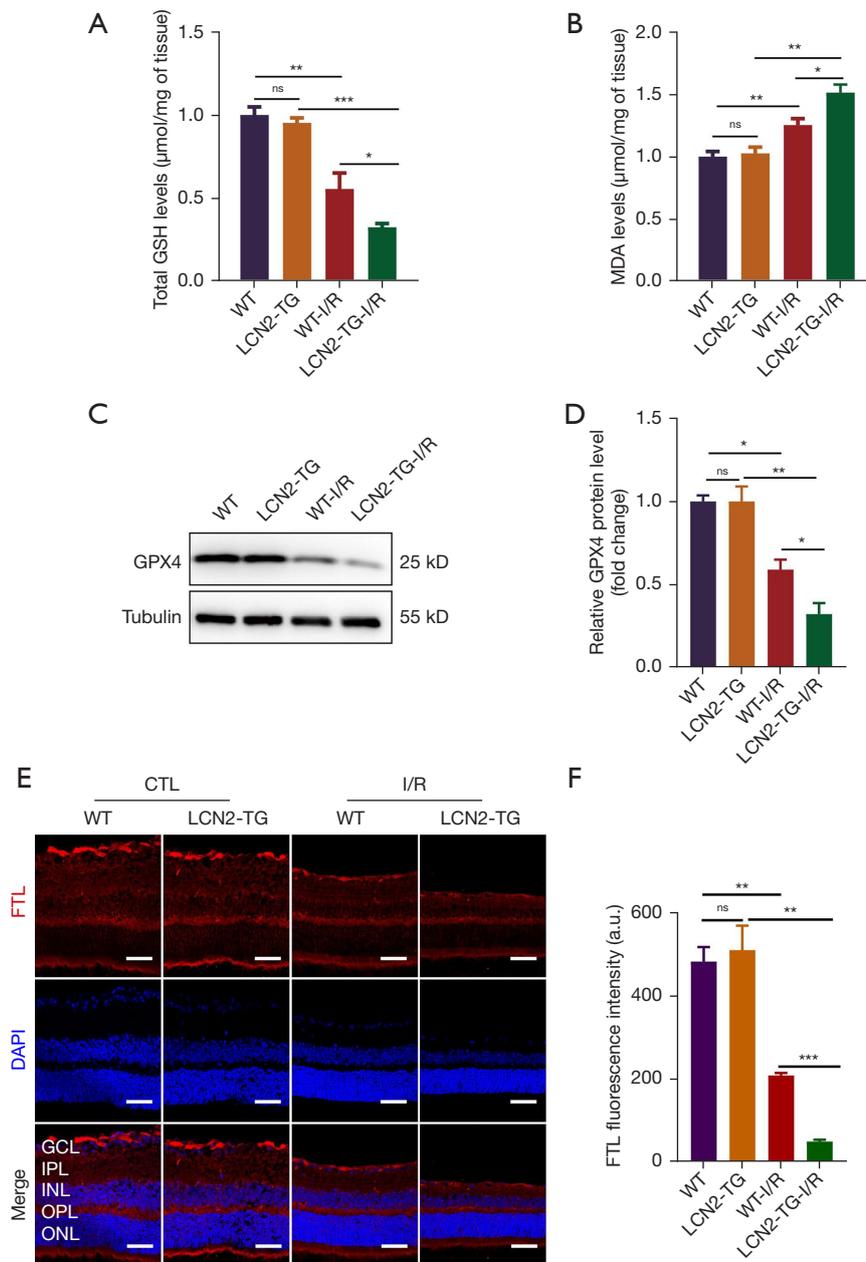
　　　　　　Ann Transl Med 2023;11(1):3 | https://dx.doi.org/10.21037/atm-22-3298

Page 8 of 15

Mei et al. LCN2 promotes ferroptosis in ischemic retinopathy

Figure 3 Upregulated LCN2 facilitated retinal ferroptosis in the retinal ischemia-reperfusion injury model. All samples were collected from the retinas 5 days after RIR injury. (A) The level of total GSH in the retina. n=10 mice per group. All data represent the mean ± SEM. *, P<0.05; **, P<0.01; ***, P<0.001; ns, no significance. Data were normalized to the weight of tissues. (B) The level of MDA in the retina. n=6 mice per group. All data represent the mean ± SEM. *, P<0.05; **, P<0.01; ns, no significance. Data were normalized to the weight of tissues. (C,D) GPX4 expression in the retina was detected using Western blotting. n=3 mice per group. All data represent the mean ± SEM. *, P<0.05; **, P<0.01; ns, no significance. Statistical analysis was performed with an unpaired 2-tailed Student *t*-test. (E,F) Representative photomicrographs of immunofluorescence staining for FTL (red) in the retina. n=3 mice per group. Scale bar: 50 μm. All data represent the mean ± SEM. **, P<0.01; ***, P<0.001; ns, no significance. Statistical analysis was performed with an unpaired 2-tailed Student *t*-test. GSH, glutathione; WT, wild-type; LCN2, lipocalin-2; LCN2-TG, LCN2 transgenic; I/R, ischemia/reperfusion; MDA, malondialdehyde; GCL, ganglion cell layer; IPL, inner plexiform layer; INL, inner nuclear layer; OPL, outer plexiform layer; ONL, outer nuclear layer; FTL, ferritin light chains; SEM, standard error of the mean.
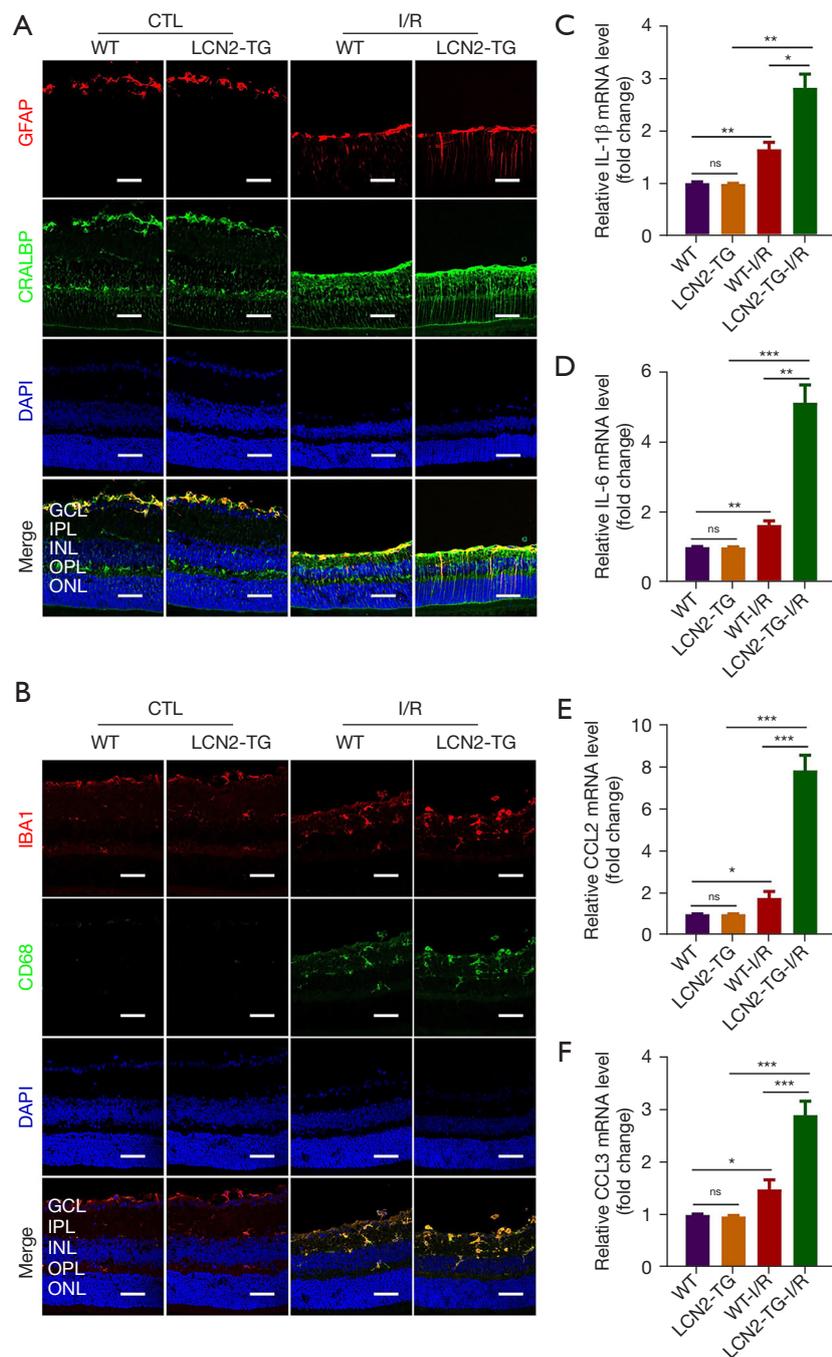
Figure 4 Upregulated LCN2 promoted activated glial cells and aggravated inflammatory responses. All samples were collected from the retinas 5 days after RIR injury. (A) Double immune staining for CRALBP (green) and GFAP (red) in the retinal sections from CTL or RIR injury group. Scale bar: 50 μm. (B) Confocal images of retinal sections showed the expression of IBA1 (red) and CD68 (green) in the retina from the CTL or RIR injury group. Scale bar: 50 μm. (C-F) RT-PCR analysis of *IL-1β*, *IL-6*, *CCL2*, and *CCL3* mRNA levels in the retinas. n=6 mice per group. All data represent the mean ± SEM. *, P<0.05; **, P<0.01; ***, P<0.001; ns, no significance. Statistical analysis was performed with an unpaired 2-tailed Student *t*-test. CTL, control; WT, wild-type; LCN2, lipocalin-2; LCN2-TG, LCN2 transgenic; I/R, ischemia/reperfusion; CRALBP, cellular retinaldehyde-binding protein; GFAP, glial fibrillary acidic protein; DAPI, 4',6-diamidino-2-phenylindole; GCL, ganglion cell layer; INL, inner nuclear layer; IPL, inner plexiform layer; ONL, outer nuclear layer; OPL, outer plexiform layer; IL-6, interleukin 6; IL-1β, interleukin 1 beta; RIR, retinal ischemia-reperfusion; SEM, standard error of the mean.

upregulated LCN2 significantly activated glial cells and microglia while inducing the expression of inflammatory cytokines, thereby exacerbating the inflammatory response.

Ferroptosis inhibitor liproxstatin-1 (LPX-1) mitigated RGC death and retinal impairment after RIR injury

Two main features of ferroptosis are iron dependency and the accumulation of lipid-reactive oxygen species (6). Elevated LCN2 could induce ferroptosis and subsequently induce retinal damage in the RIR injury model. Therefore, we used inhibitors of ferroptosis (LPX-1) to rescue RGC death and visual impairment. LPX-1, an effective ferroptosis inhibitor, has been reported to attenuate acute renal failure in mice (19,34). Intraperitoneal treatment with LPX-1 (10 mg/kg body weight) of both WT and *LCN2-TG* mice could effectively ameliorate RGC death after RIR injury compared with control groups (*Figure 5A,5B*; Figure S6A,S6B). Additionally, in the mouse retinas of the RIR injury control groups, intraperitoneal LPX-1 treatment led to remarkably increased protein levels of GPX4, which indicated that retinal ferroptosis was inhibited by LPX-1 treatment (*Figure 5C,5D*; Figure S6C,S6D). Moreover, through comparison with the control mice, we found that an apparently higher FVEP response could be triggered after RIR injury (*Figure 5E,5F*; Figure S6E,S6F). These findings demonstrated that LCN2-induced ferroptosis could be inhibited by LPX-1 and that inhibiting retinal ferroptosis could partially restore RGC death and vision function impairment in the RIR injury model.

Downregulated LCN2 alleviated RGC death and retinal impairment after RIR injury

Since overexpressed LCN2 resulted in retinal ferroptosis and aggravated RGC death and visual impairment after RIR injury, we used LCN2$^{+/-}$ knockout mice to investigate whether downregulation of LCN2 could alleviate RGC loss. The targeted allele was knocked out in exons 1–5 of *LCN2* on mouse chromosome 2 via the CRISPR/Cas9 editing system (*Figure 6A*). Compared with those in WT mice, the retinas of LCN2$^{+/-}$ mice showed a 50% decreased protein level of LCN2 (*Figure 6B*). The number of RGCs in the retina significantly increased in LCN2$^{+/-}$ mice after RIR injury (*Figure 6C,6D*). Moreover, the impairment of visual function could be remarkably ameliorated after RIR injury in LCN2$^{+/-}$ mice compared with WT mice (*Figure 6E,6F*).

These results showed that RGC death was alleviated and visual function was restored in LCN2$^{+/-}$ mice.

Discussion

RIR injury is involved in multiple forms of pathogenic processes underlying ischemic retinopathy and often causes visual impairment and irreversible blindness (35). Retinal neurons, particularly RGCs, are vulnerable to ischemia, and hypoxia leads to ganglion cell injury or loss (36). Therefore, it is necessary to understand the molecular mechanism of RGC loss and death caused by RIR injury. Doing so can provide a basis for the development of new therapies.

LCN2 belongs to the lipocalin protein family, and it is a small secretory protein (37). The expression of LCN2 shows positive correlation with elevated IOP (38). In our study, we observed that LCN2 was mainly expressed in the GCL in the retina of WT mice. Via comparison with the control group, the expression of retinal LCN2 was found to be remarkably upregulated at 1, 3, and 5 days after RIR injury (*Figure 1A,1B*). LCN2 is an early response gene in elevated IOP-induced ischemic damage models. However, whether elevated LCN2 can directly exert damaging effects in RIR injury remains largely unknown.

Although the distribution of LCN2 in the retina was obviously different between WT and *LCN2-TG* mice, there was no difference in retinal morphology between the 2 groups before RIR treatment. However, compared with those in WT mice, the retinas of *LCN2-TG* mice exhibited more grievous damage with RIR treatment. In *LCN2-TG* mice, the number of RGC and total retinal thickness significantly decreased on the fifth day after RIR injury. Vision function impairment was more severe in *LCN2-TG* mice than in controls in the RIR model. One study reported that nuclear factor kappa beta (NF-κB) and signal transducer and activator of transcription 1 (STAT1) might act together as a key promoter-binding complex in activating the expression of LCN2 in the retina at the onset of the disease state (39). Therefore, LCN2 might serve as a stress-responsive gene working in conjunction with the injury-derived signaling molecules in the RIR injury model.

A recent study using retinal explant cultures in a 2-chamber culture device indicated that LCN2 is directly involved in RGC death (40). It was further found, by exogenous administration of recombinant LCN2, that elevated LCN2 was neurotoxic to the retinal explant culture. In our study, we provided more direct evidence in
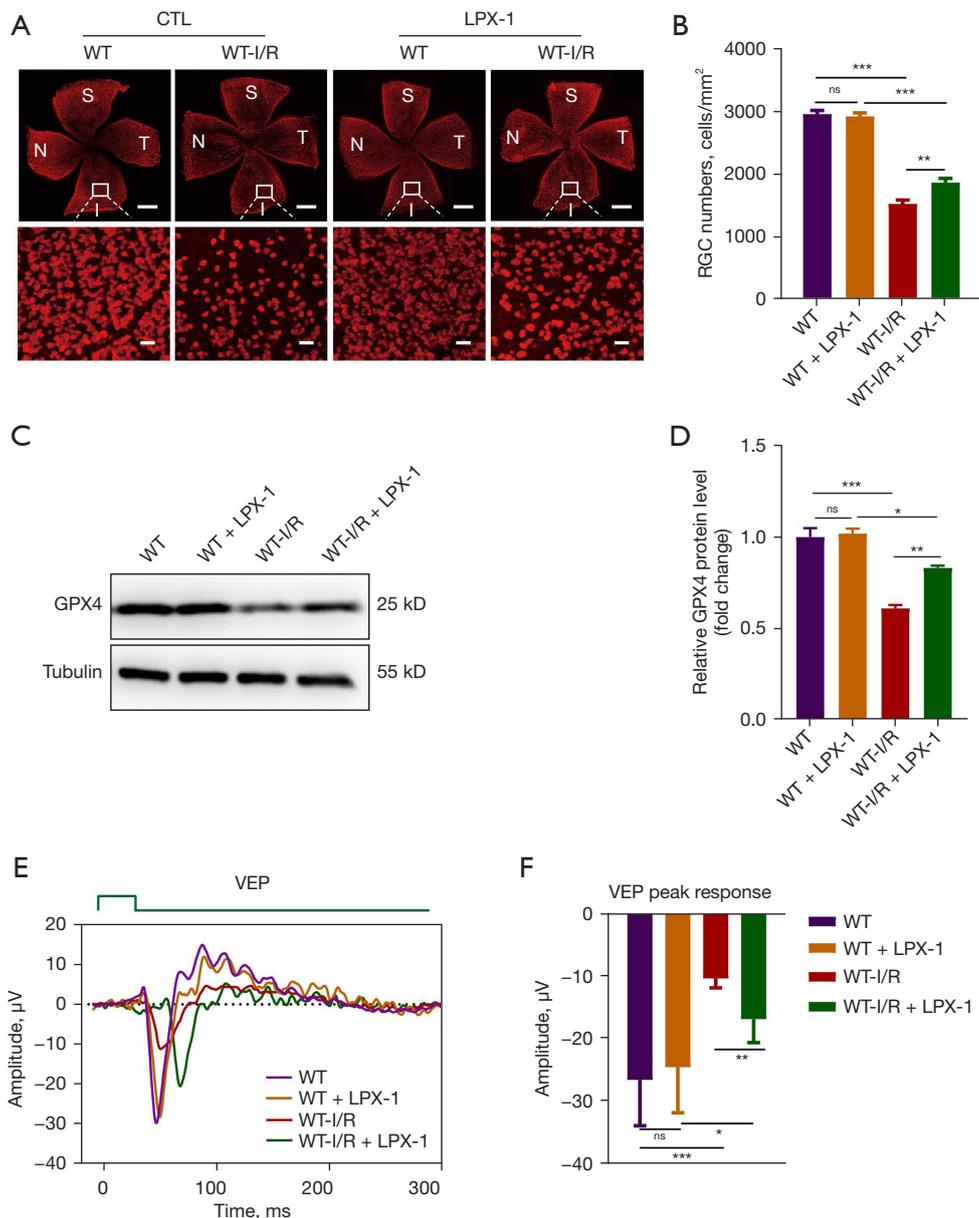
Figure 5 The ferroptosis inhibitor liproxstatin-1 mitigated RGC death and retinal impairment after RIR injury. All samples were collected from the retinas 5 days after RIR injury. (A) TissueFAXS images of retinal flat mounts showed the number of RGCs in the retina. RGCs were immunostained with an anti-RBPMS antibody. Scale bar: 500 μm (top). Scale bar: 20 μm (bottom). (B) Quantification of RGC was performed for a 200×200 μm area in 12 areas captured from the peripheral, middle, and central areas of the retina and averaged for retinas per each control and experimental condition. n=6 mice per group. All data represent the mean ± SEM. **, $P<0.01$; ***, $P<0.001$; ns, no significance. (C,D) GPX4 expression in the retina was detected by Western blotting. n=3 mice per group. All data represent the mean ± SEM. *, $P<0.05$; **, $P<0.01$; ***, $P<0.001$; ns, no significance. (E,F) VEPs of WT and WT + LPX-1 mice in left eyes (without RIR injury) and in right eyes (with RIR injury). E shows the response, and F shows the amplitudes of the VEPs response peaks. n=6 mice per group. All data represent the mean ± SEM. *, $P<0.05$; **, $P<0.01$; ***, $P<0.001$; ns, no significance. Statistical analysis was performed with an unpaired 2-tailed Student t-test. CTL, control; WT, wild-type; I/R, ischemia/reperfusion; LPX-1, liproxstatin-1; S, superior; N, nasal; I, inferior; T, temporal; RGC, retinal ganglion cell; VEP, visual evoked response; RIR, retinal ischemia-reperfusion; RBPMS, RNA-binding protein with multiple splicing; SEM, standard error of the mean.
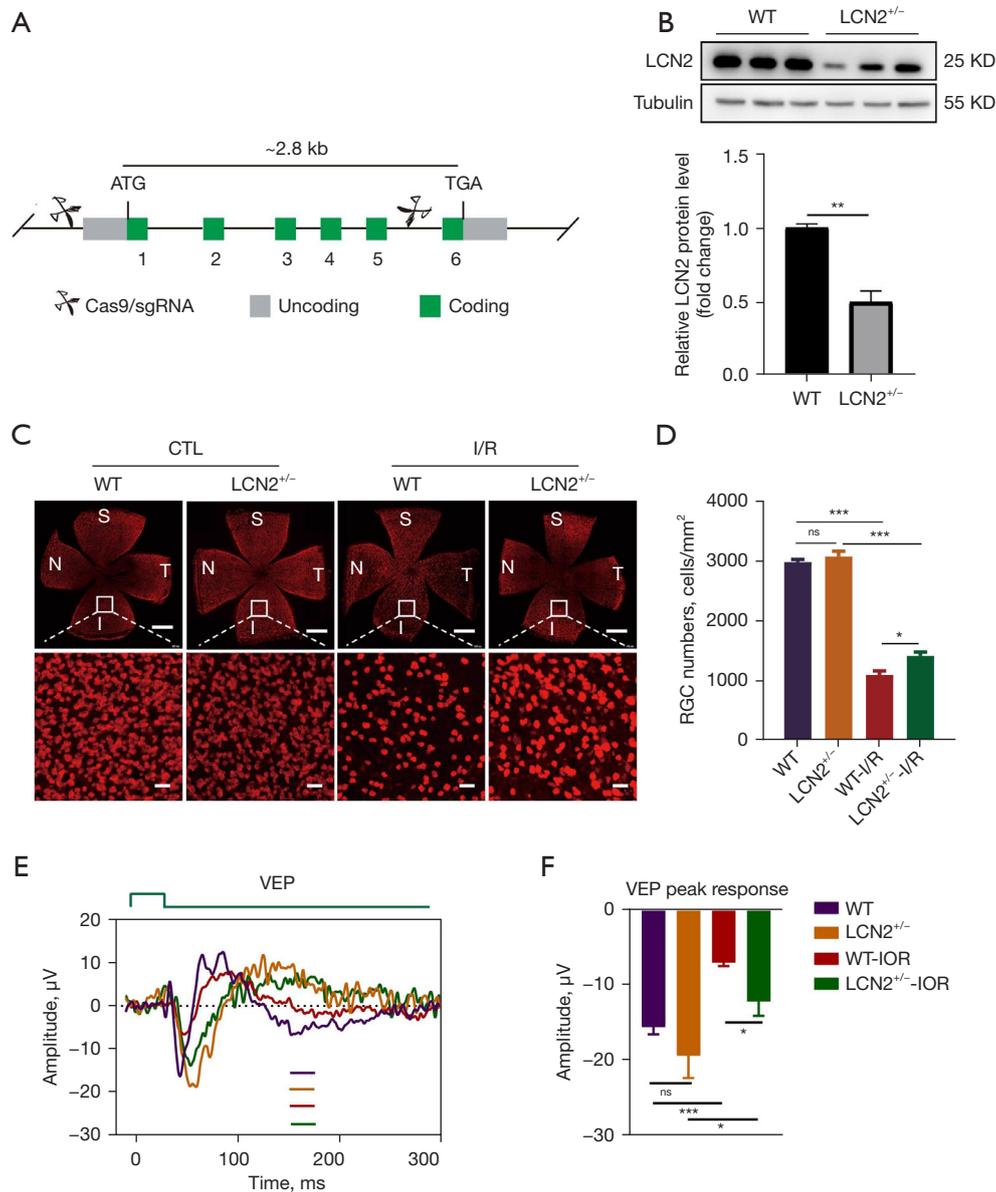
Page 12 of 15

Mei et al. LCN2 promotes ferroptosis in ischemic retinopathy

Figure 6 Downregulated LCN2 could alleviate RGC death and retinal impairment in RIR injury. All samples were collected from the retinas 5 days after RIR injury. (A) A schematic diagram of LCN2 knockout mice generated at exons 1–5 of *Lcn2* on mouse chromosome 2 via the CRISPR/Cas9 system. (B) The protein level of LCN2 in the retinas of LCN2^{+/-} mice was detected using Western blotting. n=3 mice per group. All data represent the mean ± SEM. **, P<0.01. (C) TissueFaxs images of retinal flat mounts showed the number of RGCs in the retina. RGCs were immunostained with an anti-RBPMS antibody. Scale bar: 500 µm (top). Scale bar: 20 µm (bottom). (D) Quantification of RGCs was performed for a 200×200 µm area in 4 quadrants from the peripheral, middle, and central retina and averaged for retinas per each control and experimental condition. n=4 mice per group. All data represent the mean ± SEM. *, P<0.05; ***, P<0.001; ns, no significance. (E,F) VEPs of WT and LCN2^{+/-} mice in left eyes (without RIR injury) and in right eyes (with RIR injury). (E) shows the response, and (F) shows the amplitudes of the VEPs response peaks. n=5 mice per group. All data represent the mean ± SEM. *, P<0.05; ***, P<0.001; ns, no significance. Statistical analysis was performed with an unpaired 2-tailed Student *t*-test. ATG, start codon; TGA, stop codon; WT, wild-type; LCN2, lipocalin-2; CTL, control; S, superior; N, nasal; I, inferior; T, temporal; RGC, retinal ganglion cell; VEP, visual evoked response; IOP, intraocular pressure; RIR, retinal ischemia-reperfusion; SEM, standard error of the mean; RBPMS, RNA-binding protein with multiple splicing.

that elevated LCN2 led to damaged RGC and impaired visual functions in the RIR injury model of *LCN2-TG* mice (*Figure 2*). Our studies also showed that elevated LCN2 exhibited retinal neurotoxicity by upregulating ferroptosis signaling pathways.

Ferroptosis is related to the pathogenesis of neurodegeneration, which can be induced by the low activity of the GPX4 and GSH systems in neurodegenerative diseases (10,41). Neural tissues in the brain are vulnerable to oxidative damage caused by excessive iron and lipid peroxidation (42,43). Ferroptosis is involved in the pathogenesis of blinding diseases, such as glaucoma, age-related macular degeneration, and retinitis pigmentosa (44-47). Ferroptosis was found to be enhanced in N-methyl-D-aspartate-induced RGC death (48). In our study, we showed that retinal ferroptosis could also be induced in *LCN2-TG* mice after RIR injury, as evident from the significantly decreased GSH contents, increased MDA levels, and downregulated expression of GPX4 and FTL (*Figure 3*). More importantly, our study showed that inhibiting retinal ferroptosis and downregulation of LCN2 could significantly protect against RGC death and visual impairment (*Figures 5,6*; Figure S6).

Our study found that upregulated LCN2 was involved in aggravated RGC death and visual impairment in elevated IOP-induced RIR injury mice. LCN2 exerted deleterious effects on the retina by promoting ferroptosis. These results suggest that inhibiting ferroptosis by intraperitoneal LPX-1 and downregulation of LCN2 could alleviate RGC death and visual impairment.

Conclusions

We demonstrated that LCN2 is an important regulator in promoting RGC death through ferroptosis in the retina, and overexpressed LCN2 exacerbated retinal damage and visual function impairment after RIR injury. Our study shows the connection between LCN2 and ferroptosis and their interactions with RGC degeneration, which may provide potential therapeutic targets for ischemic retinopathy.

Acknowledgments

Footnote

Reporting Checklist: The authors have completed the ARRIVE reporting checklist. Available at https://atm.amegroups.com/article/view/10.21037/atm-22-3298/rc

Data Sharing Statement: Available at https://atm.amegroups.com/article/view/10.21037/atm-22-3298/dss

Peer Review File: Available at https://atm.amegroups.com/article/view/10.21037/atm-22-3298/prf

Conflicts of Interest: All authors have completed the ICMJE uniform disclosure form (available at https://atm.amegroups.com/article/view/10.21037/atm-22-3298/coif). The authors have no conflicts of interest to declare.

Ethical Statement: The authors are accountable for all aspects of the work in ensuring that questions related to the accuracy or integrity of any part of the work are appropriately investigated and resolved. Experiments were performed under a project license (No. 2020-070) granted by the Institutional Ethics Committee of the Zhongshan Ophthalmic Center, Sun Yat-sen University, in compliance with its guidelines for the care and use of animals.

Page 14 of 15

Mei et al. LCN2 promotes ferroptosis in ischemic retinopathy

References

1. Chen H, Deng Y, Gan X, et al. NLRP12 collaborates with NLRP3 and NLRC4 to promote pyroptosis inducing ganglion cell death of acute glaucoma. Mol Neurodegener 2020;15:26.

2. Jo DH, Kim JH, Kim JH. A platform of integrative studies from in vitro to in vivo experiments: towards drug development for ischemic retinopathy. Biomed Pharmacother 2015;69:367-73.

3. Tang Y, Xiao Z, Pan L, et al. Therapeutic Targeting of Retinal Immune Microenvironment With CSF-1 Receptor Antibody Promotes Visual Function Recovery After Ischemic Optic Neuropathy. Front Immunol 2020;11:585918.

4. Fouda AY, Xu Z, Shosha E, et al. Arginase 1 promotes retinal neurovascular protection from ischemia through suppression of macrophage inflammatory responses. Cell Death Dis 2018;9:1001.

5. Toychiev AH, Batsuuri K, Srinivas M. Gap Junctional Coupling Between Retinal Astrocytes Exacerbates Neuronal Damage in Ischemia-Reperfusion Injury. Invest Ophthalmol Vis Sci 2021;62:27.

6. Dixon SJ, Lemberg KM, Lamprecht MR, et al. Ferroptosis: an iron-dependent form of nonapoptotic cell death. Cell 2012;149:1060-72.

7. Yang WS, Stockwell BR. Ferroptosis: Death by Lipid Peroxidation. Trends Cell Biol 2016;26:165-76.

8. Yang WS, SriRamaratnam R, Welsch ME, et al. Regulation of ferroptotic cancer cell death by GPX4. Cell 2014;156:317-31.

9. Liu M, Kong XY, Yao Y, et al. The critical role and molecular mechanisms of ferroptosis in antioxidant systems: a narrative review. Ann Transl Med 2022;10:368.

10. Wu JR, Tuo QZ, Lei P. Ferroptosis, a Recent Defined Form of Critical Cell Death in Neurological Disorders. J Mol Neurosci 2018;66:197-206.

11. Guiney SJ, Adlard PA, Bush AI, et al. Ferroptosis and cell death mechanisms in Parkinson's disease. Neurochem Int 2017;104:34-48.

12. Cui QN, Bargoud AR, Ross AG, et al. Oral administration of the iron chelator deferiprone protects against loss of retinal ganglion cells in a mouse model of glaucoma. Exp Eye Res 2020;193:107961.

13. Qin Q, Yu N, Gu Y, et al. Inhibiting multiple forms of cell death optimizes ganglion cells survival after retinal ischemia reperfusion injury. Cell Death Dis 2022;13:507.

14. Ferreira AC, Dá Mesquita S, Sousa JC, et al. From the periphery to the brain: Lipocalin-2, a friend or foe? Prog Neurobiol 2015;131:120-36.

15. Jha MK, Lee S, Park DH, et al. Diverse functional roles of lipocalin-2 in the central nervous system. Neurosci Biobehav Rev 2015;49:135-56.

16. Qiu S, Chen X, Pang Y, et al. Lipocalin-2 protects against renal ischemia/reperfusion injury in mice through autophagy activation mediated by HIF1α and NF-κb crosstalk. Biomed Pharmacother 2018;108:244-53.

17. Liu M, Chen J, Zhang S, et al. Downregulation of lipocalin-2 and Bim expression after remote limb preconditioning in the ischemic rat brain. Brain Res 2018;1679:1-9.

18. Skowronska-Krawczyk D, Zhao L, Zhu J, et al. P16INK4a Upregulation Mediated by SIX6 Defines Retinal Ganglion Cell Pathogenesis in Glaucoma. Mol Cell 2015;59:931-40.

19. Friedmann Angeli JP, Schneider M, Proneth B, et al. Inactivation of the ferroptosis regulator Gpx4 triggers acute renal failure in mice. Nat Cell Biol 2014;16:1180-91.

20. Ide S, Kobayashi Y, Ide K, et al. Ferroptotic stress promotes the accumulation of pro-inflammatory proximal tubular cells in maladaptive renal repair. Elife 2021;10:e68603.

21. Luo J, Zhao L, Chen AY, et al. TCF7L2 variation and proliferative diabetic retinopathy. Diabetes 2013;62:2613-7.

22. Kwong JM, Caprioli J, Piri N. RNA binding protein with multiple splicing: a new marker for retinal ganglion cells. Invest Ophthalmol Vis Sci 2010;51:1052-8.

23. Kwong JM, Quan A, Kyung H, et al. Quantitative analysis of retinal ganglion cell survival with Rbpms immunolabeling in animal models of optic neuropathies. Invest Ophthalmol Vis Sci 2011;52:9694-702.

24. Stockwell BR, Friedmann Angeli JP, Bayir H, et al. Ferroptosis: A Regulated Cell Death Nexus Linking Metabolism, Redox Biology, and Disease. Cell 2017;171:273-85.

25. Owen JB, Butterfield DA. Measurement of oxidized/reduced glutathione ratio. Methods Mol Biol 2010;648:269-77.

26. Tang H, Chen D, Li C, et al. Dual GSH-exhausting sorafenib loaded manganese-silica nanodrugs for inducing the ferroptosis of hepatocellular carcinoma cells. Int J Pharm 2019;572:118782.

27. Totsuka K, Ueta T, Uchida T, et al. Oxidative stress induces ferroptotic cell death in retinal pigment epithelial cells. Exp Eye Res 2019;181:316-24.

28. Song X, Xie Y, Kang R, et al. FANCD2 protects against

bone marrow injury from ferroptosis. Biochem Biophys Res Commun 2016;480:443-9.

29. Yang WS, Kim KJ, Gaschler MM, et al. Peroxidation of polyunsaturated fatty acids by lipoxygenases drives ferroptosis. Proc Natl Acad Sci U S A 2016;113:E4966-75.

30. Muhoberac BB, Vidal R. Iron, Ferritin, Hereditary Ferritinopathy, and Neurodegeneration. Front Neurosci 2019;13:1195.

31. Jang E, Kim JH, Lee S, et al. Phenotypic polarization of activated astrocytes: the critical role of lipocalin-2 in the classical inflammatory activation of astrocytes. J Immunol 2013;191:5204-19.

32. Jang E, Lee S, Kim JH, et al. Secreted protein lipocalin-2 promotes microglial M1 polarization. FASEB J 2013;27:1176-90.

33. Chang ML, Wu CH, Jiang-Shieh YF, et al. Reactive changes of retinal astrocytes and Müller glial cells in kainate-induced neuroexcitotoxicity. J Anat 2007;210:54-65.

34. Fan BY, Pang YL, Li WX, et al. Liproxstatin-1 is an effective inhibitor of oligodendrocyte ferroptosis induced by inhibition of glutathione peroxidase 4. Neural Regen Res 2021;16:561-6.

35. Mishra J, Mori K, Ma Q, et al. Amelioration of ischemic acute renal injury by neutrophil gelatinase-associated lipocalin. J Am Soc Nephrol 2004;15:3073-82.

36. Liu W, Xia F, Ha Y, et al. Neuroprotective Effects of HSF1 in Retinal Ischemia-Reperfusion Injury. Invest Ophthalmol Vis Sci 2019;60:965-77.

37. Dekens DW, Eisel ULM, Gouweleeuw L, et al. Lipocalin 2 as a link between ageing, risk factor conditions and age-related brain diseases. Ageing Res Rev 2021;70:101414.

38. Ueno S, Yoneshige A, Koriyama Y, et al. Early Gene Expression Profile in Retinal Ganglion Cell Layer After Optic Nerve Crush in Mice. Invest Ophthalmol Vis Sci 2018;59:370-80.

39. Ghosh S, Stepicheva N, Yazdankhah M, et al. The role of lipocalin-2 in age-related macular degeneration (AMD). Cell Mol Life Sci 2020;77:835-51.

40. Yoneshige A, Hagiyama M, Takashima Y, et al. Elevated Hydrostatic Pressure Causes Retinal Degeneration Through Upregulating Lipocalin-2. Front Cell Dev Biol 2021;9:664327.

41. Hambright WS, Fonseca RS, Chen L, et al. Ablation of ferroptosis regulator glutathione peroxidase 4 in forebrain neurons promotes cognitive impairment and neurodegeneration. Redox Biol 2017;12:8-17.

42. DeGregorio-Rocasolano N, Martí-Sistac O, Gasull T. Deciphering the Iron Side of Stroke: Neurodegeneration at the Crossroads Between Iron Dyshomeostasis, Excitotoxicity, and Ferroptosis. Front Neurosci 2019;13:85.

43. Levy D, Reichert CO, Bydlowski SP. Paraoxonases Activities and Polymorphisms in Elderly and Old-Age Diseases: An Overview. Antioxidants (Basel) 2019.

44. Obolensky A, Berenshtein E, Lederman M, et al. Zinc-desferrioxamine attenuates retinal degeneration in the rd10 mouse model of retinitis pigmentosa. Free Radic Biol Med 2011;51:1482-91.

45. Wang K, Peng B, Xiao J, et al. Iron-Chelating Drugs Enhance Cone Photoreceptor Survival in a Mouse Model of Retinitis Pigmentosa. Invest Ophthalmol Vis Sci 2017;58:5287-97.

46. Yao F, Peng J, Zhang E, et al. Pathologically high intraocular pressure disturbs normal iron homeostasis and leads to retinal ganglion cell ferroptosis in glaucoma. Cell Death Differ 2022. [Epub ahead of print]. doi: 10.1038/s41418-022-01046-4.

47. Gupta U, Ghosh S, Wallace CT, et al. Increased LCN2 (lipocalin 2) in the RPE decreases autophagy and activates inflammasome-ferroptosis processes in a mouse model of dry AMD. Autophagy 2022. [Epub ahead of print]. doi: 10.1080/15548627.2022.2062887.

48. Zhou Y, Que KT, Zhang Z, et al. Iron overloaded polarizes macrophage to proinflammation phenotype through ROS/acetyl-p53 pathway. Cancer Med 2018;7:4012-22.